Title

Structure of human factor VIIa-soluble tissue factor with calcium, magnesium and rubidium.

Journal

Acta Crystallographica Section D: Structural Biology, 77(Pt 6)

Authors

Vadivel, Kanagasabai
Schmidt, Amy
Cascio, Duilio
et al.

Publication Date

2021-06-01

DOI

10.1107/S2059798321003922

Peer reviewed

STRUCTURAL BIOLOGY

ISSN 2059-7983

Structure of human factor VIIa–soluble tissue factor with calcium, magnesium and rubidium

Kanagasabai Vadivel,[a] Amy E. Schmidt,[b] Duilio Cascio,[c] Kaillathe Padmanabhan,[d] Sriram Krishnaswamy,[e] Hans Brandstetter[f] and S. Paul Bajaj[a,g]*

[a]Department of Orthopaedic Surgery, University of California, Los Angeles, CA 90095, USA, [b]Department of Pathology and Laboratory Medicine, University of Rochester Medical Center, Rochester, NY 14642, USA, [c]DOE Institute for Genomics and Proteomics, University of California, Los Angeles, CA 90095, USA, [d]Department of Biochemistry, Michigan State University, East Lansing, MI 48824, USA, [e]Division of Hematology, The Children's Hospital of Philadelphia University of Pennsylvania Perelman School of Medicine, Philadelphia, PA 19104, USA, [f]Department of Biosciences, University of Salzburg, 5020 Salzburg, Austria, and [g]Molecular Biology Institute, University of California, Los Angeles, CA 90095, USA. *Correspondence e-mail: pbajaj@mednet.ucla.edu

Received 3 November 2020
Accepted 12 April 2021

Edited by R. J. Read, University of Cambridge, United Kingdom

Keywords: blood coagulation factor VIIa; rubidium; calcium; magnesium; sodium.

PDB reference: factor VIIa–soluble tissue factor complex, 4ibl

Supporting information: this article has supporting information at journals.iucr.org/d

Coagulation factor VIIa (FVIIa) consists of a γ-carboxyglutamic acid (GLA) domain, two epidermal growth factor-like (EGF) domains and a protease domain. FVIIa binds three Mg^{2+} ions and four Ca^{2+} ions in the GLA domain, one Ca^{2+} ion in the EGF1 domain and one Ca^{2+} ion in the protease domain. Further, FVIIa contains an Na^{+} site in the protease domain. Since Na^{+} and water share the same number of electrons, Na^{+} sites in proteins are difficult to distinguish from waters in X-ray structures. Here, to verify the Na^{+} site in FVIIa, the structure of the FVIIa–soluble tissue factor (TF) complex was solved at 1.8 Å resolution containing Mg^{2+}, Ca^{2+} and Rb^{+} ions. In this structure, Rb^{+} replaced two Ca^{2+} sites in the GLA domain and occupied three non-metal sites in the protease domain. However, Rb^{+} was not detected at the expected Na^{+} site. In kinetic experiments, Na^{+} increased the amidolytic activity of FVIIa towards the synthetic substrate S-2288 (H-D-Ile-Pro-Arg-*p*-nitroanilide) by ~20-fold; however, in the presence of Ca^{2+}, Na^{+} had a negligible effect. Ca^{2+} increased the hydrolytic activity of FVIIa towards S-2288 by ~60-fold in the absence of Na^{+} and by ~82-fold in the presence of Na^{+}. In molecular-dynamics simulations, Na^{+} stabilized the two Na^{+}-binding loops (the 184-loop and 220-loop) and the TF-binding region spanning residues 163–180. Ca^{2+} stabilized the Ca^{2+}-binding loop (the 70-loop) and Na^{+}-binding loops but not the TF-binding region. Na^{+} and Ca^{2+} together stabilized both the Na^{+}-binding and Ca^{2+}-binding loops and the TF-binding region. Previously, Rb^{+} has been used to define the Na^{+} site in thrombin; however, it was unsuccessful in detecting the Na^{+} site in FVIIa. A conceivable explanation for this observation is provided.

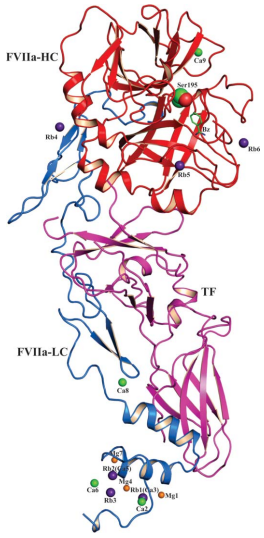

1. Introduction

Human factor VII (FVII) is a vitamin K-dependent plasma protein that is synthesized by hepatocytes and secreted into the blood as a single-chain molecule with a molecular weight of ~50 000 (Broze & Majerus, 1980; Bajaj *et al.*, 1981). FVII consists of an N-terminal γ-carboxyglutamic acid (GLA) domain, a short hydrophobic segment, two epidermal growth factor-like (EGF) domains and a C-terminal serine protease module, which consists of two β-barrel subdomains (Davie *et al.*, 1991). Several coagulation enzymes, including FXa, FIXa and FVIIa, activate FVII (Radcliffe & Nemerson, 1976; Bajaj *et al.*, 1981; Masys *et al.*, 1982; Davie *et al.*, 1991; Yamamoto *et al.*, 1992; Neuenschwander *et al.*, 1993; Butenas & Mann, 1996). In each case, activation of FVII involves the cleavage of a single peptide bond between Arg152 and Ile153 located in the connecting region between the EGF2 and protease domains. This cleavage results in the formation of a two-chain

Table 1
Data-collection and refinement statistics.

Values in parentheses are for the outer shell.

PDB code	4ibl
Data collection	
Beamline	ALS beamline 5.0.2
Wavelength (Å)	0.8153
Resolution (Å)	68.24–1.80
Molecules per asymmetric unit	1
Measured reflections	654882
Unique reflections	128119
Completeness (%)	99.8 (100.0)
Multiplicity	5.1
R_{merge}	0.075 (0.566)
Average $I/\sigma(I)$	16.6 (2.9)
Space group	$P2_12_12_1$
a, b, c (Å)	69.90, 81.06, 126.42
Refinement statistics	
Resolution (Å)	1.80
No. of non-H atoms	
Protein	4691
Ion	17
Ligand	30
Water	529
R	0.176
R_{free}	0.215
R.m.s.d.s from ideal values	
Bond lengths (Å)	0.024
Bond angles (°)	1.972
Average B factor (Å^2)	23
Ramachandran plot	
Most favoured regions (%)	88.7
Additional allowed regions (%)	11.1
Generously allowed regions (%)	0.0
Disallowed regions (%)	0.2

FVIIa that consists of an N-terminal 152-residue light chain and a C-terminal 254-residue heavy chain (serine protease domain) held together by a single disulfide bond. Upon binding to tissue factor (TF), a transmembrane protein, FVIIa activates FIX to FIXa and FX to FXa during extrinsic coagulation (Davie *et al.*, 1991). Similar to full-length TF, soluble TF (sTF) binds to FVIIa with high affinity and potentiates its enzymatic activity (Ruf *et al.*, 1991; Waxman *et al.*, 1992; Neuenschwander & Morrissey, 1992).

Crystal structures of the FVIIa–sTF complex revealed that FVIIa has multiple metal-binding sites. In the absence of Mg^{2+} the GLA domain contains seven Ca^{2+}-binding sites (Banner *et al.*, 1996), and in the presence of Mg^{2+} three specific Ca^{2+} sites are replaced by Mg^{2+} (Bajaj *et al.*, 2006; Vadivel *et al.*, 2013). The EGF1 domain and the protease domain each contain one Ca^{2+}-binding site (Banner *et al.*, 1996; Bajaj *et al.*, 2006). In addition to a Ca^{2+}-binding site, the protease domain also contains an Na^+-binding site (Bajaj *et al.*, 2006). Sequence similarity (Dang & Di Cera, 1996) predicts that the Na^+-binding site in FVIIa is similar to those in FXa (Zhang & Tulinsky, 1997), activated protein C (APC; Schmidt *et al.*, 2002) and FIXa (Vadivel *et al.*, 2019) but not to that in thrombin (Di Cera *et al.*, 1995; Zhang & Tulinsky, 1997).

In this report, we solved the structure of the FVIIa–sTF complex in the presence of Ca^{2+}, Mg^{2+} and Rb^+ to examine whether Rb^+ can be used to identify the Na^+ site in FVIIa. We performed hydrolysis of the synthetic substrate S-2288 (H-D-Ile-Pro-Arg-*p*-nitroanilide) in the presence and absence of Na^+ and Ca^{2+} to investigate the kinetic effects of these metals on the activity of FVIIa. Further, we performed molecular-dynamics (MD) simulations to investigate the role of Na^+ and Ca^{2+} in inducing structural stability in the protease domain of FVIIa.

2. Materials and methods

2.1. Expression and purification

Human FVII was expressed using the pMon3360b expression vector in BHK/VP16 cells, as described by Hippenmeyer & Highkin (1993) and Zhong *et al.* (2002). FVII was purified using a Ca^{2+}-dependent monoclonal antibody and FPLC Mono Q column chromatography (Zhong *et al.*, 2002). Purified FVII contained nine GLA residues per molecule, as measured by the procedure of Price *et al.* (1976), and appeared to be homogeneous on both reduced and nonreduced SDS–PAGE, with a molecular weight of ∼57 000. FVIIa was obtained using FXa-Sepharose as described previously, and the resin was removed by gentle centrifugation (Bajaj *et al.*, 1981; Zhong *et al.*, 2002). The purified protein was concentrated to ∼20 mg ml^{-1} and stored at −80°C until use. sTF (residues 1–219) was obtained from Tom Girard (Washington University, St Louis, Missouri, USA). sTF was concentrated to ∼10 mg ml^{-1} and stored at −80°C. Both proteins were ∼98% pure as judged by SDS–gel electrophoresis (Laemmli, 1970).

2.2. Crystallization and data collection

The benzamidine–FVIIa–sTF complex was crystallized using the hanging-drop vapour-diffusion method. Specifically, the protein drop consisted of 4 mg ml^{-1} FVIIa–sTF complex, 20 m*M* Tris–HCl pH 7.5, 200 m*M* RbCl, 10 m*M* $CaCl_2$, 10 m*M* benzamidine, whereas the reservoir solution consisted of 16–22% PEG 4000, 100 m*M* $MgCl_2$, 20 m*M* bis-Tris pH 6.5. Drops were prepared by mixing 2 µl protein solution with 2 µl reservoir solution at 20°C. Crystals appeared within seven days and were allowed to grow for 14–20 days before being flash-cooled without additional cryoprotectant. Diffraction data were collected to 1.8 Å resolution at a wavelength near the Rb absorption *K* edge on beamline 5.0.2 at the Advanced Light Source (ALS), Lawrence Berkeley National Laboratory.

2.3. Structure determination

Data indexing, integration and scaling were performed using the *HKL*-2000 suite (Otwinowski & Minor, 1997) and the crystal structure was solved by molecular replacement with *AMoRe* (Navaza, 1994) using the structure of the FVIIa–sTF complex (PDB entry 3th2; Vadivel *et al.*, 2013) as the starting model. Model building was performed using *Coot* (Emsley *et al.*, 2010) and refinement and validation were performed with the *CCP*4 suite (Collaborative Computational Project, Number 4, 1994; Winn *et al.*, 2011; Murshudov *et al.*, 2011). The Rb^+ sites were identified by calculating the anomalous difference Fourier map using the *CCP*4 suite and the Ca^{2+} sites were identified by analyzing the Fourier difference maps. Data-processing and refinement statistics are given in Table 1.

The coordinates and structure factors have been deposited in the Protein Data Bank (Berman *et al.*, 2000) as PDB entry 4ibl.

2.4. Measurement of the S-2288 amidolytic activity of FVIIa

The concentration of FVIIa used was between 0.1 and 5 µ*M*. The concentration of S-2288 (DiaPharma) ranged from 50 µ*M* to 20 m*M*. The buffer used was 50 m*M* Tris–HCl pH 7.4 containing 0.1% PEG and various salt combinations as given in the legends to the appropriate figures. Choline (Ch^+), a larger monovalent cation, was used to keep the ionic strength constant at 0.2 *M*. *p*-Nitroanilide (*p*NA) release was measured continuously ($\Delta A_{405\ nm}\ min^{-1}$) for up to 30 min using a SpectraMax 190 plate reader from Molecular Devices. An extinction coefficient of 9.9 $mM^{-1}\ cm^{-1}$ at 405 n*M* was used to calculate the amount of *p*NA released (Lottenberg & Jackson, 1983). The data were processed using nonlinear least-squares regression analysis with the Marquardt algorithm (Bevington & Robinson, 1992) and the quality of the fit was evaluated using the described criterion (Straume & Johnson, 1992). The fitted parameters are given ±95% confidence limits. Initial velocity measurements of S-2288 hydrolysis were analyzed using the Henri–Michaelis–Menten equation (Segal, 1975) to yield K_m and V_{max} values.

2.5. Global analysis of initial velocity data

The equilibrium dissociation constants for the binding of the synthetic substrate S-2288 ($K_{E,S}$), Na^+ ($K_{E,N}$) and Ca^{2+} ($K_{E,C}$) to free FVIIa, for the binding of Na^+ to substrate-bound ($K_{ES,N}$) or Ca^{2+}-bound ($K_{EC,N}$) FVIIa, for the binding of Ca^{2+} to substrate-bound ($K_{ES,C}$) or Na^+-bound ($K_{EN,C}$) FVIIa, for the binding of substrate to Na^+-bound ($K_{EN,S}$) or Ca^{2+}-bound ($K_{EC,S}$) FVIIa, for the binding of Na^+ to substrate- and Ca^{2+}-bound FVIIa ($K_{ECS,N}$), for the binding of Ca^{2+} to substrate- and Na^+-bound FVIIa ($K_{ENS,C}$) and for the binding of substrate to Na^+- and Ca^{2+}-bound FVIIa ($K_{ENC,S}$) were calculated from initial velocity measurements of S-2288 hydrolysis according to the system of common differential equations described in Fig. 1 and using the rapid equilibrium assumption. The entire data set was globally fitted using *DynaFit* (Kuzmič, 2009) to extract all of the above equilibrium dissociation constants as well as the k_{catE}, k_{catEN}, k_{catEC} and k_{catENC} values. Here, N stands for Na^+, C for Ca^{2+}, S for substrate, P for product and E for the FVIIa enzyme.

2.6. Determination of K_{dpAB} for *p*-aminobenzamidine (*p*AB) binding to FVIIa

The K_{dpAB} for *p*AB binding to FVIIa was determined by its ability to competitively inhibit S-2288 hydrolysis in the absence and presence of Na^+ with or without Ca^{2+}. Each reaction mixture contained 0.1–5 µ*M* FVIIa and 1 m*M* S-2288 in 50 m*M* Tris–HCl pH 7.4 in four varying Na^+/Ca^{2+} conditions: (i) 200 m*M* ChCl/1 m*M* EDTA, (ii) 200 m*M* NaCl/1 m*M* EDTA, (iii) 185 m*M* ChCl/5 m*M* $CaCl_2$ and (iv) 185 m*M* NaCl/5 m*M* $CaCl_2$. The IC_{50} (the concentration of *p*AB required for 50% inhibition) was determined by fitting the data to the IC_{50} four-parameter logistic equation of Halfman (1981),

$$y = \frac{a}{1 + \left(\dfrac{x}{IC_{50}}\right)^s}, \tag{1}$$

where y is the rate of *p*NA release in the presence of a given concentration of *p*AB represented by x, a is the maximum rate of *p*NA release in the absence of *p*AB, and s is the slope factor. Each point was weighted equally and the data were fitted to (1) using the nonlinear regression analysis program *GraFit* from Erithcus Software. To obtain K_{dpAB} values for the interaction of *p*AB with FVIIa, we used the following equation, as described by Cheng & Prusoff (1973) and further elaborated by Craig (1993),

$$K_d = \frac{IC_{50}}{1 + \left(\dfrac{[S]}{K_m}\right)}, \tag{2}$$

where [S] is the S-2288 concentration and K_m is the value obtained under the different conditions used to obtain K_{dpAB}.

2.7. Molecular-dynamics (MD) simulations

MD simulations were performed to investigate the effect of Na^+ and Ca^{2+} binding to the protease domain of FVIIa. MD simulations were carried out in the absence and presence of Na^+ or Ca^{2+} or of Na^+ and Ca^{2+} using the *AMBER*18 program (Case *et al.*, 2019). The FVIIa protease domain containing residues Val16 (chymotrypsin numbering; 153 in FVIIa) to Pro257 (406 in FVIIa) was used in these studies. Since the effect of Na^+ and Ca^{2+} binding to the protease domain is being

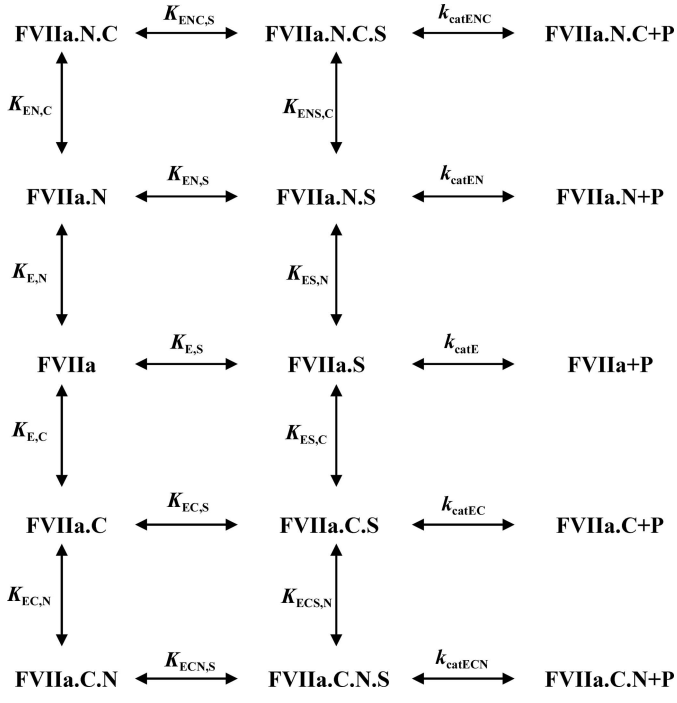

Figure 1
Equations and parameters for S-2288 hydrolysis.

evaluated, we used only the protease domain of FVIIa in these studies. After adding H atoms, the protein structures were solvated in a truncated octahedral TIP3P box of 12 Å and the system was neutralized with chloride ions. Periodic boundary conditions, particle mesh Ewald summation and *SHAKE*-enabled 2 fs time steps were used in all MD simulations. Langevin dynamics temperature control was employed with a collision rate equal to 1.0 ps^{-1}. A cutoff of 13 Å was used for nonbonding interactions. The divalent and monovalent metal-ion parameters used were taken from Li & Merz (2014) and Li *et al.* (2015) and the metal interactions were treated using the 12–6–4 Lennard–Jones nonbonded model. The initial configurations were subjected to a 1000-step minimization with harmonic constraints of 10 kcal mol^{-1} $Å^{-2}$ on the protein heavy atoms. The systems were gradually heated from 0 to 300 K over a period of 50 ps with harmonic constraints. The simulations at 300 K were then continued for 50 ps, during which the harmonic constraints were gradually lifted. The systems were then equilibrated for a period of 500 ps before the 50 ns production runs. All simulations were carried out in the NPT ensemble. Equilibration and production run simulations were carried out using the *Sander* and *PMEMD* modules (optimized for CUDA) of *AMBER*18.0 (ff14SB), respectively (Le Grand *et al.*, 2013; Case *et al.*, 2019). The initial structures of the production runs were used as reference structures for calculation of the root-mean-square deviations (r.m.s.d.s) and root-mean-square fluctuations (r.m.s.f.s). All analyses were performed using the *cpptraj* module of *AmberTools*18 (Case *et al.*, 2019).

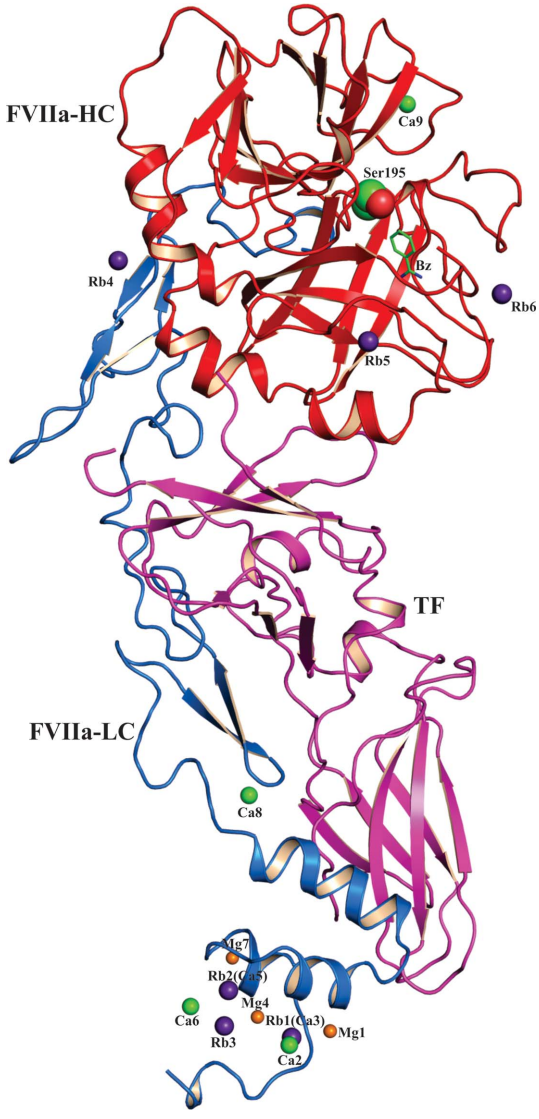

Figure 2
Structure of the FVIIa–sTF complex. Cartoon representation of the FVIIa–sTF structure obtained with Ca^{2+}, Mg^{2+} and Rb^{+}. The FVIIa light chain is in blue and the heavy chain is in red. sTF is shown in magenta. The active-site residue Ser195 is shown in space-filling representation and benzamidine (Bz) bound at the active site is shown in stick representation. The Ca^{2+}, Mg^{2+} and Rb^{+} ions bound to FVIIa are shown as green, orange and purple spheres, respectively. Note that the Ca^{2+} ions at positions 3 and 5 are replaced by Rb1 and Rb2, respectively.

3. Results

3.1. Structure of FVIIa–sTF

The FVIIa–sTF complex was crystallized in the presence of Ca^{2+}, Mg^{2+} and Rb^{+} and the data were collected near the Rb *K* absorption edge. The FVIIa–sTF structure was determined by molecular replacement and the structure is similar to previous FVIIa–sTF complex structures. Based upon the Rb anomalous signal, three Rb^{+} ions were found in the GLA domain and three in the protease domain (Fig. 2). The refined occupancies for the Rb^{+} ions were 0.65 (Rb1), 0.65 (Rb2), 0.75 (Rb3), 0.55 (Rb4), 0.48 (Rb5) and 0.50 (Rb6), and the *B* factors were 48, 55, 32, 46, 52 and 46 $Å^2$, respectively. Two of the three Rb^{+} ions in the GLA domain occupied the Ca^{2+}-binding sites at positions 3 and 5 (the metal-binding site numbering in the GLA domain is based on Soriano-Garcia *et al.*, 1992) and the third site was found on the surface. The coordination geometry of the identified Rb^{+} ions in FVIIa are shown in Fig. 3. Moreover, although three Rb^{+} ions were identified in the protease domain, none of them was found at the putative Na^{+} site and each is surface-bound.

3.2. Effects of monovalent cations on the amidolytic activity of FVIIa

Our initial efforts were directed towards finding an inert monovalent cation that could be used to keep the ionic strength constant during the kinetic experiments. Hydrolysis of S-2288 by FVIIa was measured at various concentrations of Rb^{+}, Cs^{+} or choline (Ch^{+}) as inert monovalent cations. Rb^{+}, Cs^{+} or Ch^{+} did not inhibit or potentiate the amidolytic activity of FVIIa (Fig. 4*a*). Further, Na^{+} potentiated the amidolytic activity of FVIIa to a similar extent whether or not Ch^{+} was present (Fig. 4*b*). Thus, Ch^{+} was used as the compensatory ion in subsequent experiments.

3.3. Effect of Na^{+} and Ca^{2+} on the potentiation of S-2288 hydrolysis by FVIIa

The enhancement of substrate-hydrolysis activity by various concentrations of Na^{+} or Ca^{2+} at varying concentrations of

S-2288 is shown in Figs. 5(*a*) and 5(*b*), respectively. Similarly, the enhancement of substrate-hydrolysis activity at varying concentrations of Ca^{2+} in the presence of constant Na^+ (200 m*M*) or at varying concentrations of Na^+ in the presence of constant Ca^{2+} (5 m*M*) is depicted in Figs. 5(*c*) and 5(*d*), respectively. The entire data set was globally fitted using *DynaFit* according to Fig. 1, and the calculated parameters are given in Table 2. The binding of Na^+ to FVIIa had no effect on the S-2288 substrate affinity; however, it increased the k_{cat} ~21.4-fold. Conversely, the binding of Ca^{2+} to FVIIa decreased the affinity of the substrate by ~3.7-fold but increased the k_{cat} by ~231-fold. Na^+ binding to Ca^{2+}-bound FVIIa had little effect on the substrate affinity or the k_{cat} (Tables 2 and 3). Further, Ca^{2+} binding to Na^+-bound FVIIa decreased the affinity of the substrate by ~3.3-fold and increased the k_{cat} by ~12.4-fold. Cumulatively, these data suggest that Na^+ has relatively little effect on the affinity of FVIIa for substrate but considerably increases the k_{cat} in the absence of Ca^{2+}. However, Na^+ has essentially no effect on the substrate affinity or k_{cat} in the presence of Ca^{2+}. In contrast, Ca^{2+} decreases the affinity of FVIIa for substrate and substantially increases the k_{cat} in the absence or presence of Na^+ (Tables 2 and 3). The conclusions from the global fitting approach were independently verified by initial velocity studies of peptidyl substrate cleavage at near-saturating concentrations of Ca^{2+} and/or Na^+. There was good agreement between the steady-state kinetic constants determined under these conditions (Table 3) and those inferred from the global analysis (Table 2).

3.4. Molecular-dynamics studies

To investigate the role of Na^+ in FVIIa, we performed MD simulations on the FVIIa protease domain for 50 ns each in the presence of Na^+, Ca^{2+} or of Na^+ and Ca^{2+} as well as in the absence of these metals using the *AMBER*18 package (Case *et al.*, 2019). The r.m.s.d. and the average r.m.s.f. for the backbone atoms of the FVIIa protease domain for the 50 ns MD data are presented in Fig. 6. The MD data indicate that the presence of Na^+, Ca^{2+} or of Na^+ and Ca^{2+} stabilizes the FVIIa protease domain compared with the metal-free form (Fig. 6*a*). The average r.m.s.f. for the backbone atoms of each residue presented in Fig. 6(*b*) indicate that Na^+ reduces residue fluctuations (~0.75 Å) in the two Na^+-binding loops (184-loop, residues 183–194; 220-loop, residues 216–225) as well as in the tissue factor-binding region (residues 163–180), while Ca^{2+} reduces fluctuations (~0.5 Å) in the Ca^{2+}-binding loop residues (residues 70–80) as well as in the Na^+-binding loops. The presence of both Ca^{2+} and Na^+ reduces fluctuations in the Ca^{2+}-binding loop (~0.6 Å) and the two Na^+-binding loops (~0.75 Å; residues 183–194 and residues 216–225) as well as

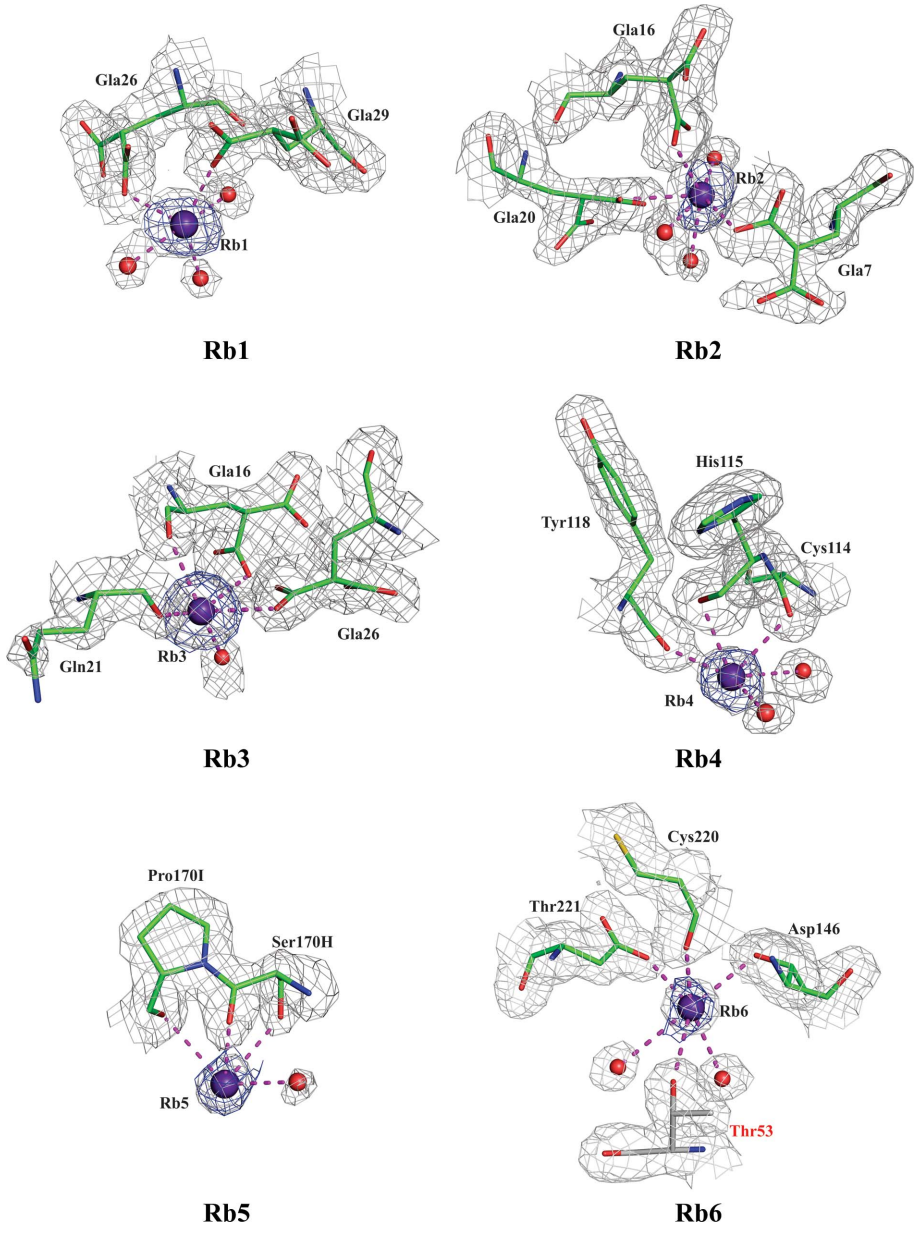

Figure 3
Coordination geometries of Rb^+ sites in the FVIIa–sTF structure. The residues coordinated to Rb^+ are shown in stick representation. The electron-density ($2F_{obs} - F_{calc}$) maps (black) are contoured at 1σ and the anomalous maps (in blue) for Rb^+ are contoured at 3σ. C atoms are green, N atoms are blue and O atoms are red. The C atoms are coloured grey in the residue coordinated to Rb^+ from the symmetry-related molecule. The Rb^+ ions and water molecules are shown as purple and red spheres, respectively. The residues coordinated to Rb4, Rb5 and Rb6 are in the protease domain and are labelled with chymotrypsin numbering.

Table 2
Parameters for Fig. 1 determined by global fit analysis.

Note that the value of $K_{ENC,S}$ is the same as that of $K_{ECN,S}$ and that the value of k_{catECN} is the same as that of k_{catENC}.

Parameter	Fitted value
$K_{E,S}$ (m*M*)	1.9 ± 0.3
$K_{EN,S}$ (m*M*)	2.4 ± 0.4
$K_{EC,S}$ (m*M*)	9.4 ± 0.7
$K_{ENC,S}$ (m*M*)	8.2 ± 0.9
$K_{E,N}$ (m*M*)	160 ± 30
$K_{ES,N}$ (m*M*)	155 ± 32†
$K_{EC,N}$ (m*M*)	168 ± 41‡
$K_{ECS,N}$ (m*M*)	149 ± 35§
$K_{E,C}$ (m*M*)	0.20 ± 0.05
$K_{ES,C}$ (m*M*)	0.81 ± 0.20¶
$K_{EN,C}$ (m*M*)	0.52 ± 0.16
$K_{ENS,C}$ (m*M*)	1.87 ± 0.43††
k_{catE} (min^{-1})	0.8 ± 0.2
k_{catEN} (min^{-1})	21.9 ± 1.8
k_{catEC} (min^{-1})	215.2 ± 24.1
k_{catENC} (min^{-1})	257.1 ± 32.5

† $K_{ES,N}$ was obtained using $K_{E,N}(K_{EN,S}/K_{E,S})$ ‡ $K_{EC,N}$ was obtained using $K_{E,N}(K_{EN,C}/K_{E,C})$. § $K_{ECS,N}$ was obtained using $K_{ES,N}(K_{ENS,C}/K_{ES,C})$. ¶ $K_{ES,C}$ was obtained using $K_{E,C}(K_{EC,S}/K_{E,S})$. †† $K_{ENS,C}$ was obtained using $K_{EN,C}(K_{ENC,S}/K_{EN,S})$.

Table 3
Effect of Na^+ and Ca^{2+} on the hydrolysis of S-2288 by FVIIa.

To keep the ionic strength constant, Ch^+ was used at 200 m*M* in the absence of Na^+ and Ca^{2+}. The concentration of Na^+ was 200 m*M* in the absence of Ca^{2+} and 185 m*M* in the presence of 5 m*M* Ca^{2+}. The buffer used was 50 m*M* Tris pH 7.4 containing 0.1% PEG 8000. The results presented are the average of three experiments ± SE.

Conditions				
Na^+	Ca^{2+}	K_m (m*M*)	k_{cat} (min^{-1})	k_{cat}/K_m† (min^{-1} mM^{-1})
—	—	2.4 ± 0.4	0.9 ± 0.1	0.4 (1)†
+	—	2.2 ± 0.3	19.3 ± 0.9	8.8 (22)
—	+	8.8 ± 1.3	207.7 ± 15	23.6 (59)
+	+	7.8 ± 0.7	239.9 ± 10	32.8 (82)

† The fold change in the specificity constant k_{cat}/K_m is given in parentheses.

the tissue factor-binding region (∼1.0 Å; residues 163–180). Cumulatively, the MD data suggest that Na^+ plays a role in stabilizing the two Na^+-binding loops and the tissue factor-binding region in the FVIIa protease domain.

4. Discussion and conclusion

Dang & Di Cera (1996) compared the sequences of serine proteases and classified them into two classes: proteases with Pro225 that lack the Na^+ site and proteases with Tyr225 or Phe225 that possess the Na^+ site. As per the Dang and Di Cera classification, the coagulation proteases thrombin, FVIIa, FIXa and FXa, as well as APC and complement C1r and C1s, which carry Tyr225 or Phe225, bind Na^+, while trypsin, chymotrypsin, elastase, FXIa, FXIIa, kallikrein, urokinase and plasmin, which carry Pro225, do not bind Na^+. Accordingly, synthetic substrate hydrolysis by thrombin, FIXa, FXa and APC is allosterically enhanced by Na^+ binding (Orthner & Kosow, 1978, 1980; Steiner & Castellino, 1985; Dang *et al.*, 1995; Dang & Di Cera, 1996; He & Rezaie, 1999; Rezaie & He, 2000; Underwood *et al.*, 2000; Schmidt *et al.*, 2002, 2005). Further, the residue 225 specificity of Na^+ binding in thrombin (Dang & Di Cera, 1996) and FIXa (Schmidt *et al.*, 2005) has been demonstrated by mutating Tyr225 to Pro: enhancement of synthetic substrate hydrolysis by Na^+ was impaired by a Tyr225Pro mutation in both enzymes.

Identification of the metal-binding sites in proteins is important in order to understand their functions in biology. The extensive work of Marjorie Harding on metal-binding sites in proteins provides a framework to define and identify metal ions in protein structures (Harding, 1999, 2000, 2002, 2004, 2006; Harding *et al.*, 2010). Her analysis of the metal–ligand interactions in protein structures and comparisons with the Cambridge Structural Database (CSD; Groom *et al.*, 2016) for ligands that are analogues of amino-acid side chains in proteins provide guidelines for metal–donor atom distances,

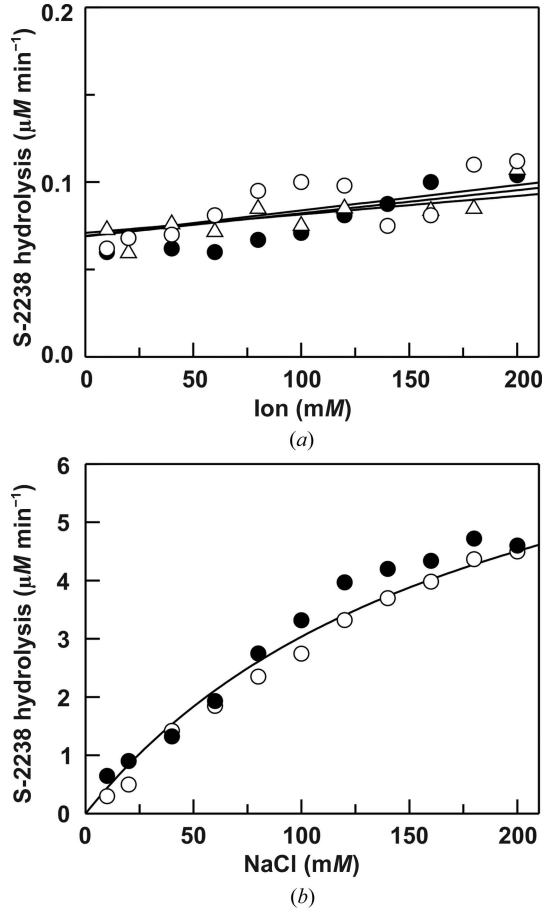

Figure 4
Effect of monovalent cations on the amidolytic activity of FVIIa. (*a*) Effect of Rb^+, Cs^+ or Ch^+ on the amidolytic activity of FVIIa. Reaction mixtures consisted of 1 m*M* S-2288 and 1 μ*M* FVIIa in 50 m*M* Tris pH 7.4, 0.1% PEG 8000, 1 m*M* EDTA and various concentrations of either Rb^+ (closed circles), Cs^+ (open triangles) or Ch^+ (open circles). The chloride salt of each ion was used. (*b*) Effect of Na^+ on the amidolytic activity of FVIIa. The buffer conditions are the same as in (*a*). Open circles represent an experiment where increasing concentrations of Na^+ were used in the absence of a compensating monovalent ion. Closed circles represent an experiment where the monovalent cation concentration was kept constant at 0.2 *M* by the addition of Ch^+ as a compensating ion.

coordination numbers and the extent of distortion from the ideal geometry. Harding's analyses further define the architecture of metal-coordination groups in proteins and their preferences for Na, Mg, K, Ca, Mn, Fe, Co, Ni, Cu and Zn metal cations. Among these cations, the interactions between Na^+ and ligand atoms from the protein or water molecules are more electrostatic and to some extent less covalent in nature; thus, it is difficult to precisely define the interaction distances for Na^+ (Harding, 2006). Although the ideal coordination distance for Na^+ is 2.38 ± 0.10 Å, this is not always the case in protein structures. In many instances, the distances are longer and there are fewer than six coordinate ligand atoms (Harding, 2002), which necessitates additional documentation to unequivocally define Na^+ sites in proteins.

Furthermore, the crystallographic identification of Na^+ in proteins is not straightforward due to the comparable electron density of a water molecule and the Na^+ ion (Stubbs & Bode, 1993). In this context, enhancement of thrombin activity by Na^+ was observed in 1980 (Orthner & Kosow, 1980); however, the Na^+ site was not crystallographically defined until 1995 (Di Cera *et al.*, 1995). It was the work of Di Cera *et al.* (1995) and Zhang & Tulinsky (1997) that identified the Na^+ site by

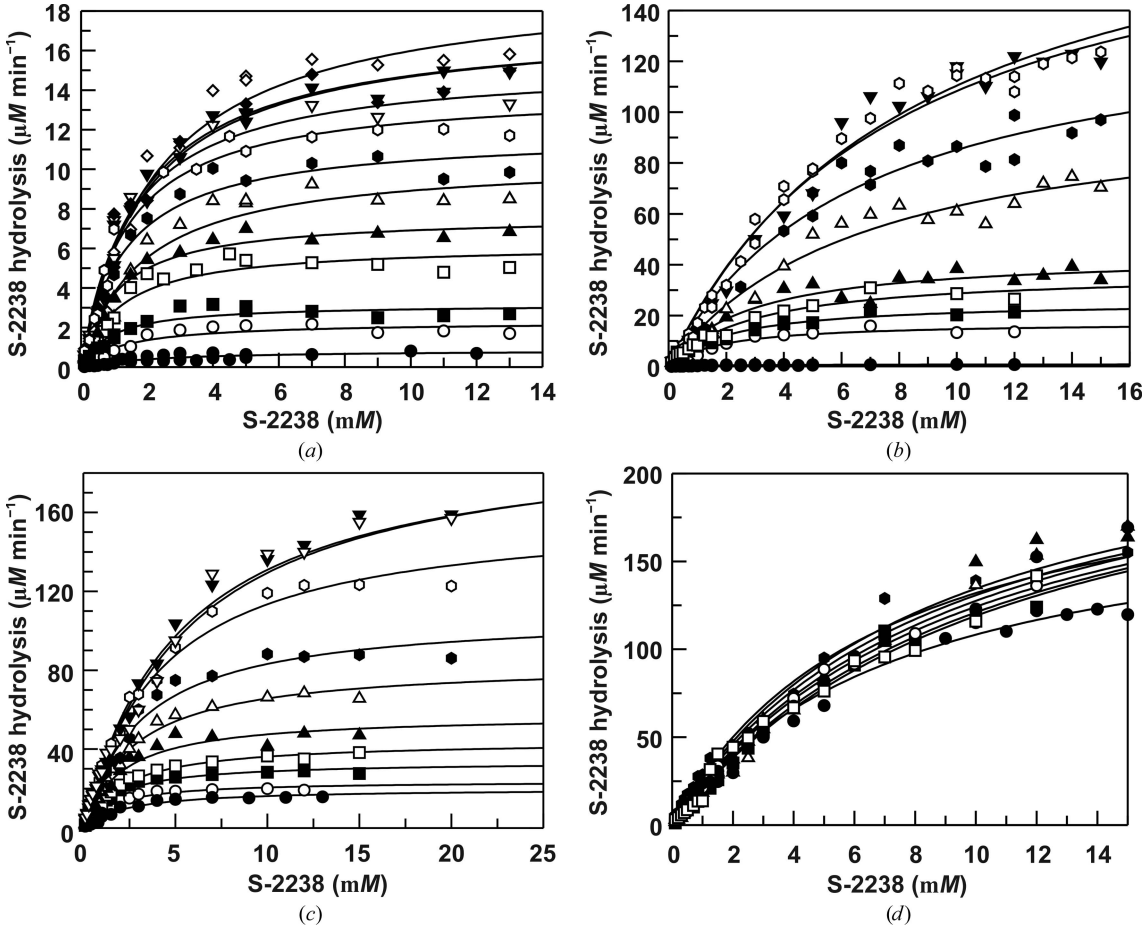

Figure 5
Na^+- and Ca^{2+}-mediated potentiation of S-2288 hydrolysis by FVIIa. (*a*) Na^+-mediated potentiation of S-2288 hydrolysis by FVIIa in the absence of Ca^{2+}. Monovalent ion concentrations are 0 m*M* Na^+/200 m*M* Ch^+ (closed circles), 10 m*M* Na^+/190 m*M* Ch^+ (open circles), 25 m*M* Na^+/175 m*M* Ch^+ (closed squares), 50 m*M* Na^+/150 m*M* Ch^+ (open squares), 75 m*M* Na^+/125 m*M* Ch^+ (closed triangles), 100 m*M* Na^+/100 m*M* Ch^+ (open triangles), 125 m*M* Na^+/75 m*M* Ch^+ (closed hexagons), 150 m*M* Na^+/50 m*M* Ch^+ (open hexagons), 165 m*M* Na^+/35 m*M* Ch^+ (closed inverted triangles), 175 m*M* Na^+/25 m*M* Ch^+ (open inverted triangles), 190 m*M* Na^+/10 m*M* Ch^+ (closed diamonds) and 200 m*M* Na^+/0 m*M* Ch^+ (open diamonds). The concentration of FVIIa used was from 0.1 to 5 μ*M*; for consistency, the data were normalized to 1 μ*M* enzyme concentration. (*b*) Ca^{2+}-mediated potentiation of S-2288 hydrolysis by FVIIa in the absence of Na^+. Ca^{2+} concentrations are 0 m*M* (closed circles), 25 μ*M* (open circles), 50 μ*M* (closed squares), 0.10 m*M* (open squares), 0.25 m*M* (closed triangles), 0.50 m*M* (open triangles), 1.0 m*M* (closed hexagons), 3.0 m*M* (open hexagons) and 5.0 m*M* (closed inverted triangles). The ionic strength was kept constant in each reaction mixture by adding 185–200 m*M* Ch^+. The FVIIa concentrations used were 0.1–5 μ*M*. As in (*a*), the data were normalized to 1 μ*M* FVIIa concentration. (*c*) Ca^{2+}-mediated potentiation of S-2288 hydrolysis by FVIIa in the presence of Na^+. Ca^{2+} concentrations are 0 m*M* (closed circles), 25 μ*M* (open circles), 50 μ*M* (closed squares), 0.10 m*M* (open squares), 0.25 m*M* (closed triangles), 0.50 m*M* (open triangles), 1 m*M* (closed hexagons), 2.0 m*M* (open hexagons), 3.0 m*M* (closed inverted triangles) and 5.0 m*M* (open inverted triangles). The concentration of Na^+ in each case was 185 m*M*, and the Ch^+ concentration was varied to keep the ionic strength constant. The FVIIa concentrations used were 0.1–5 μ*M* and were normalized to 1 μ*M* as in (*a*) and (*b*). (*d*) Na^+-mediated potentiation of S-2288 hydrolysis by FVIIa in the presence of Ca^{2+}. Na^+ concentrations are 0 m*M* (closed circles), 25 m*M* (open circles), 50 m*M* (closed squares), 75 m*M* (open squares), 100 m*M* (closed triangles), 125 m*M* (open triangles), 150 m*M* (closed diamonds) and 185 m*M* (closed hexagons). Each reaction mixture contained 5 m*M* Ca^{2+} and an appropriate concentration of Ch^+ to maintain a constant ionic strength. The concentration of FVIIa used was 0.1 μ*M*, which was normalized to 1 μ*M* as in (*a*) and (*b*). All lines are drawn following global analysis according to Fig. 1 using the fitted values in Table 2.

soaking thrombin crystals with Rb^+. The Rb^+–thrombin structure revealed the location of the Na^+ ion and its coordination to the main-chain carbonyl O atoms of residues 221A and 224 and four water molecules. This is represented schematically in Fig. 7(*a*). Based on the location of the Na^+ site in thrombin, Zhang & Tulinsky (1997) re-examined the structure of FXa (Padmanabhan *et al.*, 1993), found a water molecule coordinated to four carbonyl O atoms and correctly replaced it with Na^+. The Na^+ ion at this site in FXa is coordinated to the main-chain carbonyl O atoms of residues 184A, 185, 221A and 224 and two water molecules (Zhang & Tulinsky, 1997). Later, Schmidt *et al.* (2002), Bajaj *et al.* (2006) and Vadivel *et al.* (2019) reported that Na^+ at a similar site in APC, FVIIa and FIXa, respectively, is coordinated to four carbonyl O atoms (Fig. 7*b*) and two water molecules. A four-residue insertion in the 184-loop of thrombin prevents the participation of the 184-loop in Na^+ binding (Fig. 7*a*).

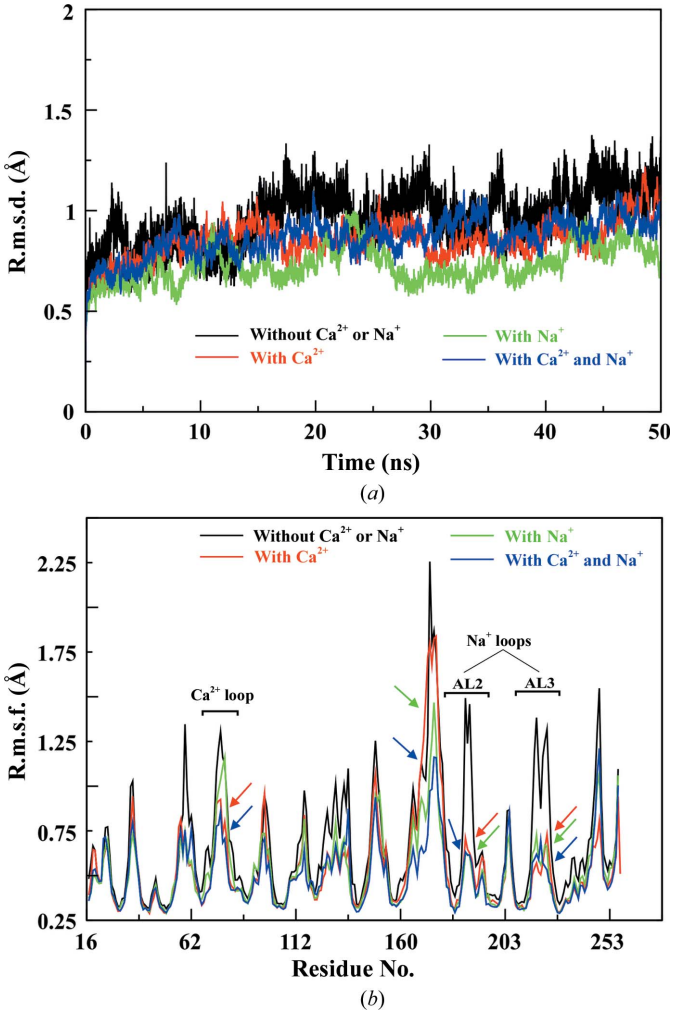

Figure 6
The r.m.s.d. and the average r.m.s.f. of the backbone atoms of the FVIIa protease domain in the absence as well as the presence of Na^+, of Ca^{2+} or of Na^+ and Ca^{2+}. (*a*) R.m.s.d. of backbone atoms of FVIIa over 50 ns MD trajectories. (*b*) Comparative r.m.s.f. plots of the backbone atoms of FVIIa during 50 ns MD simulations. In both (*a*) and (*b*) black represents the absence of Na^+ and Ca^{2+}, green represents the presence of Na^+, red represents the presence of Ca^{2+} and blue represents the presence of both Na^+ and Ca^{2+}. Arrows in (*b*) indicate the reduced fluctuations in the residues of the Ca^{2+} and Na^+ loops in the presence of Na^+ or Ca^{2+} as well as of both Na^+ and Ca^{2+}.

As found for FIXa (Dang & Di Cera, 1996; Schmidt *et al.*, 2005; Gopalakrishna & Rezaie, 2006), Na^+ enhances synthetic substrate hydrolysis by FVIIa in the absence of Ca^{2+} and has essentially no effect in the presence of Ca^{2+} (Fig. 5; Petrovan & Ruf, 2000). In contrast, Na^+ enhances synthetic substrate hydrolysis by FXa (Orthner & Kosow, 1978; Rezaie & He, 2000; Underwood *et al.*, 2000) and APC (Steiner & Castellino, 1985; He & Rezaie, 1999; Schmidt *et al.*, 2002) in the absence or presence of Ca^{2+}. Further, in Ca^{2+}-containing buffers, Na^+ had a minimal effect on the interaction of FXa with FVa (Camire, 2002), of FIXa with FVIIIa (Schmidt *et al.*, 2005) and of FVIIa with TF (Petrovan & Ruf, 2000; Bajaj *et al.*, 2006). Na^+ also had a minimal effect on the activation of prothrombin by FXa/FVa (Camire, 2002), of FX by FIXa/FVIIIa (Schmidt *et al.*, 2005; Gopalakrishna & Rezaie, 2006) and of FX by FVIIa/TF (Petrovan & Ruf, 2000; Gopalakrishna & Rezaie, 2006). Whether or not Na^+ plays a role in the inactivation of FVa or FVIIIa by APC/protein S has not been investigated. Thus, it would appear that the respective cofactor in the cases of FVIIa, FIXa or FXa eliminates the need for Na^+ for optimal biological activity. Further work is required to establish the role of Na^+ in the inactivation of FVa or FVIIIa by APC/protein S.

In the MD simulations, compared with free FVIIa, Na^+ stabilized the Na^+-binding loops and the TF-binding region, whereas Ca^{2+} stabilized the Ca^{2+}-binding loop and the Na^+-binding loops but not the TF-binding region. Thus, Na^+ contributes in part towards stabilization of the FVIIa protease domain. In this context, it is particularly interesting to re-investigate crystal structures of FVIIa which were determined in the absence of TF, particularly PDB entries 1klj and 1kli, which both lack an Na^+ ion at the expected Na^+-binding site (Sichler *et al.*, 2002). While the absence of an Na^+ ion in PDB entry 1klj is consistent with its limited resolution of 2.44 Å, the data set for PDB entry 1kli, which was determined at 1.7 Å resolution, deserves a more careful analysis. Indeed, the relevant solvent structure is intriguing. According to the PDB entry 1kli coordinate set, a water molecule is positioned in the neighbourhood of the three carbonyls of Tyr184, Thr221 and His224. Such a three-carbonyl oxygen coordination is inconsistent with an ordered water molecule, but is consistent with a Na^+ ion. Furthermore, current structure-refinement protocols, including the automatic *PDB-REDO* (Joosten *et al.*, 2011, 2014), reveal significant positive difference electron density at more than 5σ above the mean. Consequently, a reanalysis with current refinement protocols strongly favours the presence of an Na^+ ion in FVIIa in the absence of TF (Fig. 8).

Notably, structural identification of the Na^+ site in thrombin was determined by soaking the crystals with Rb^+ (Di Cera *et al.*, 1995). Here, we made a similar effort to identify the Na^+ site in FVIIa using Rb^+ as a probe. However, unlike thrombin, Rb^+ did not occupy the Na^+ site in the FVIIa protease domain. A possible explanation for the absence of Rb^+ occupancy at the Na^+ site in FVIIa is that the exact composition of the Na^+ site differs between FVIIa and thrombin. The Na^+ site in

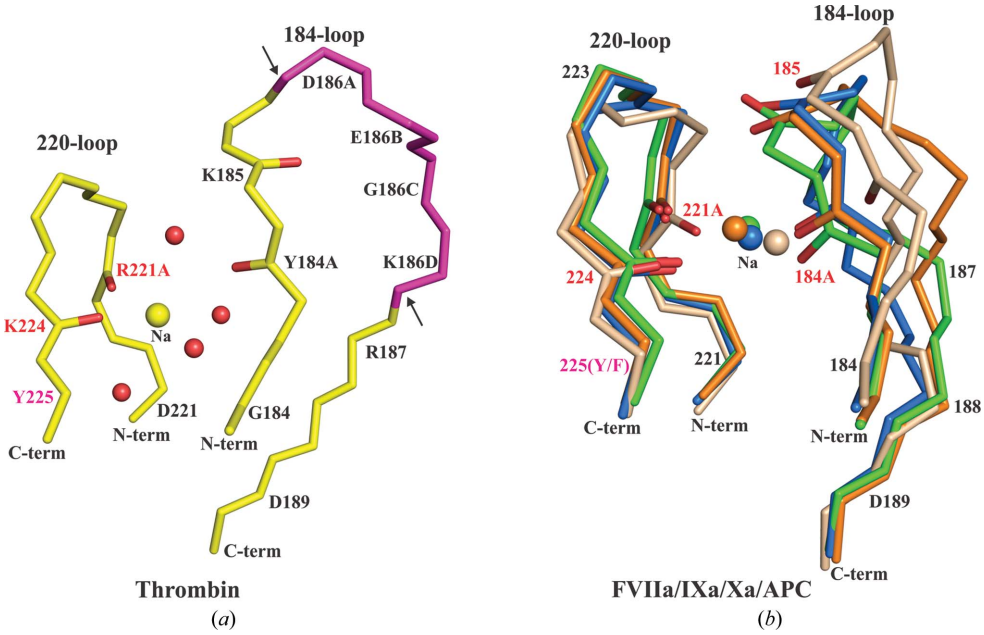

Figure 7
Comparison of the Na^+-binding site between thrombin and FVIIa, FIXa, FXa and APC. (*a*) The Na^+-binding site of thrombin. Two of the main-chain carbonyl O atoms (Arg221A and Lys224) of the 220-loop and four water molecules, which serve as ligands for Na^+, are shown. Only the backbone atoms, without the carbonyl O atoms, except for those that serve as ligands for the Na^+ ion, are shown in stick representation. The Na^+ ions (yellow) and water molecules (red) are shown as spheres. (*b*) The Na^+-binding sites in FVIIa (green), FIXa (blue), FXa (orange) and APC (wheat). The main-chain carbonyl O atoms from both the 184-loop (184A and 185) and the 220-loop (221A and 224) residues serve as ligands for Na^+. As in (*a*), only the backbone atoms, without the carbonyl O atoms, except for those that serve as ligands for Na^+, are shown in stick representation. The Na^+ ion is shown as a green sphere for FVIIa, a blue sphere for FIXa, an orange sphere for FXa and a wheat sphere for APC. For clarity, the two water molecules that also coordinate to Na^+ in these proteases are not shown.

thrombin is located in the prominent water channel filled with more than 20 highly conserved water molecules linked together by a hydrogen-bond network that also connects to the protein (Zhang & Tulinsky, 1997). Four water molecules in this solvent channel and two carbonyl O atoms from the 220-loop coordinate to Na^+ in thrombin. Notably, the Na^+ site in thrombin is deep and is exposed to the surface, which allows Rb^+ to occupy the Na^+ site even though Rb^+ has a larger ionic radius (1.52 Å; Shannon, 1976) and requires a longer

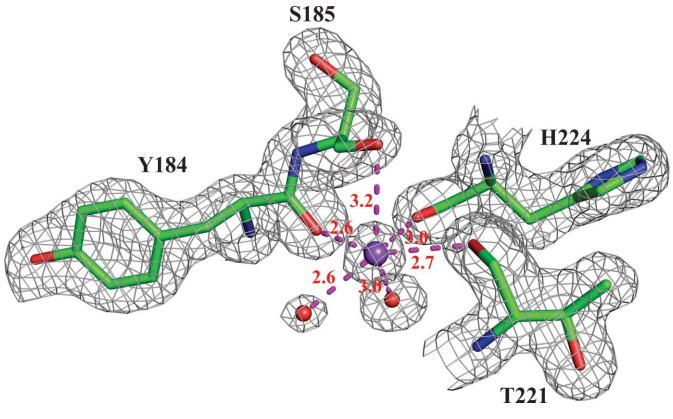

Figure 8
The Na^+ site in the FVIIa protease domain in the absence of TF (PDB entry 1kli). The carbonyl O atoms of FVIIa residues Tyr184, Ser185, Thr221 and His224 and the two water molecules that serve as ligands for Na^+ are shown. The electron-density ($2F_{obs} - F_{calc}$) map is contoured at 1σ. The Na^+ ion and water molecules are shown as purple and red spheres, respectively.

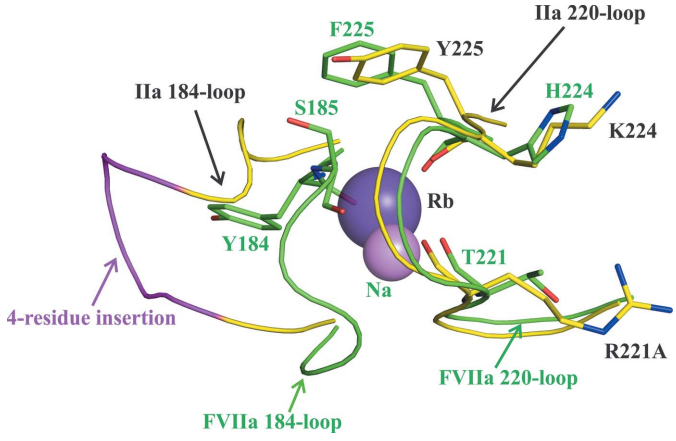

Figure 9
Comparison of the molecular environment of the Na^+ site in FVIIa and thrombin. In FVIIa, residues from both the 184-loop and the 220-loop (Tyr184, Ser185, Thr221 and His224) participate in coordinating to Na^+, whereas in thrombin only residues from the 220-loop (Arg221A and Lys224) are involved. The spatial restraints imposed by the 184-loop and 220-loop prevent Rb^+ occupancy at the Na^+ site in FVIIa. The Na^+ and Rb^+ ions are shown as pink and purple spheres, respectively. The ionic radii of Na^+ (1.02 Å) and Rb^+ (1.52 Å) were used to draw the spheres (Shannon, 1976). The residues that serve as ligands for Na^+ are shown in stick representation. Residue 225, which defines the presence of a Na^+ site in these proteases, is also shown in stick representation. The FVIIa loops are shown in green and the thrombin loops are in yellow. The four-residue insertion in the 184-loop of thrombin is shown in magenta.

coordination distance compared with Na^+ (ionic radius of 1.02 Å). The ideal coordination distance for Rb–O is 2.98 Å (it varies between 2.7 and 3.2 Å in small molecules; Groom *et al.*, 2016) as determined using large-angle X-ray scattering and extended X-ray absorption fine structure studies (D'Angelo & Persson, 2004). Similar to in small molecules, the Rb^+ coordination distance varies between 2.7 and 3.6 Å in proteins (Zhang & Tulinsky, 1997; Berman *et al.*, 2000; Korolev *et al.*, 2001). Comparatively, the Na^+ coordination distance varies from 2.4 to 3.01 Å in proteins (Harding, 2002). Accordingly, Rb^+ occupancy at the Na^+ site in thrombin results in the rearrangement of water molecules as well as the involvement of the 184-loop residue Tyr184A. Compared with thrombin, the absence of a four-residue insertion in the 184-loop of FVIIa leads to four carbonyl O atoms (Tyr184, Ser185, Thr221 and His224) from the 184-loop and 220-loop and two water molecules coordinating to Na^+. Consequently, the Na^+ site in FVIIa is narrow and is not exposed to the surface. Thus, spatial restraints imposed by the 184-loop and 220-loop in FVIIa prevent Rb^+ occupancy at the Na^+ site due to its larger ionic radius compared with Na^+ (Fig. 9). This is consistent with the previous finding that Rb^+ does not always occupy the Na^+ site in macromolecules, especially in less exposed and narrow spaces (Machius *et al.*, 1998; Nonaka *et al.*, 2003). Thus, the molecular environment of the Na^+ site in a protein determines whether Rb^+ can occupy the Na^+ site. Overall, the analysis points out that the Na^+ site in FVIIa is similar to those in FIXa, FXa and APC but not to that in thrombin.

Acknowledgements

We thank Dr Michael Sawaya and the UCLA–DOE X-ray Crystallization and Crystallography Core Facilities (supported by Department of Energy grant DE-FC02-02ER63421) for assistance with crystallization and data collection.

Funding information

This work was supported in part by National Heart, Lung and Blood Institute grants R01HL141850 to SPB, P01HL139420 to SK and by Austrian Science Fund FWF project No. W1213 to HB.

References

Bajaj, S. P., Rapaport, S. I. & Brown, S. F. (1981). *J. Biol. Chem.* **256**, 253–259.
Bajaj, S. P., Schmidt, A. E., Agah, S., Bajaj, M. S. & Padmanabhan, K. (2006). *J. Biol. Chem.* **281**, 24873–24888.
Banner, D. W., D'Arcy, A., Chène, C., Winkler, F. K., Guha, A., Konigsberg, W. H., Nemerson, Y. & Kirchhofer, D. (1996). *Nature*, **380**, 41–46.
Berman, H. M., Westbrook, J., Feng, Z., Gilliland, G., Bhat, T. N., Weissig, H., Shindyalov, I. N. & Bourne, P. E. (2000). *Nucleic Acids Res.* **28**, 235–242.
Bevington, P. R. & Robinson, K. D. (1992). *Data Reduction and Error Analysis for the Physical Sciences*. New York: McGraw–Hill.
Broze, G. J. Jr & Majerus, P. W. (1980). *J. Biol. Chem.* **255**, 1242–1247.
Butenas, S. & Mann, K. G. (1996). *Biochemistry*, **35**, 1904–1910.
Camire, R. M. (2002). *J. Biol. Chem.* **277**, 37863–37870.
Case, D. A., Ben-Shalom, I. Y., Brozell, S. R., Cerutti, D. S., Cheatham, T. E. III, Cruzeiro, V. W. D., Darden, T. A., Duke, R. E., Ghoreishi, D., Gilson, M. K., Gohlke, H., Goetz, A. W., Greene, D., Harris, R., Homeyer, N., Izadi, S., Kovalenko, A., Kurtzman, T., Lee, T. S., LeGrand, S., Li, P., Lin, C., Liu, J., Luchko, T., Luo, R., Mermelstein, D. J., Merz, K. M., Miao, Y., Monard, G., Nguyen, C., Nguyen, H., Omelyan, I., Onufriev, A., Pan, F., Qi, R., Roe, D. R., Roitberg, A., Sagui, C., Schott-Verdugo, S., Shen, J., Simmerling, C. L., Smith, J., Salomon-Ferrer, R., Swails, J., Walker, R. C., Wang, J., Wei, H., Wilson, L., Wolf, R. M., Wu, X., Xiao, L., Xiong, Y., York, D. M. & Kollman, P. A. (2019). *AMBER*2019. University of California, San Francisco, USA.
Cheng, Y.-C. & Prusoff, W. H. (1973). *Biochem. Pharmacol.* **22**, 3099–3108.
Collaborative Computational Project, Number 4 (1994). *Acta Cryst.* D**50**, 760–763.
Craig, D. A. (1993). *Trends Pharmacol. Sci.* **14**, 89–91.
Dang, Q. D. & Di Cera, E. (1996). *Proc. Natl Acad. Sci. USA*, **93**, 10653–10656.
Dang, Q. D., Vindigni, A. & Di Cera, E. (1995). *Proc. Natl Acad. Sci. USA*, **92**, 5977–5981.
D'Angelo, P. & Persson, I. (2004). *Inorg. Chem.* **43**, 3543–3549.
Davie, E. W., Fujikawa, K. & Kisiel, W. (1991). *Biochemistry*, **30**, 10363–10370.
Di Cera, E., Guinto, E. R., Vindigni, A., Dang, Q. D., Ayala, Y. M., Wuyi, M. & Tulinsky, A. (1995). *J. Biol. Chem.* **270**, 22089–22092.
Emsley, P., Lohkamp, B., Scott, W. G. & Cowtan, K. (2010). *Acta Cryst.* D**66**, 486–501.
Gopalakrishna, K. & Rezaie, A. R. (2006). *Thromb. Haemost.* **95**, 936–941.
Groom, C. R., Bruno, I. J., Lightfoot, M. P. & Ward, S. C. (2016). *Acta Cryst.* B**72**, 171–179.
Halfman, C. J. (1981). *Methods Enzymol.* **74**, 481–497.
Harding, M. M. (1999). *Acta Cryst.* D**55**, 1432–1443.
Harding, M. M. (2000). *Acta Cryst.* D**56**, 857–867.
Harding, M. M. (2002). *Acta Cryst.* D**58**, 872–874.
Harding, M. M. (2004). *Acta Cryst.* D**60**, 849–859.
Harding, M. M. (2006). *Acta Cryst.* D**62**, 678–682.
Harding, M. M., Nowicki, M. W. & Walkinshaw, M. D. (2010). *Crystallogr. Rev.* **16**, 247–302.
He, X. & Rezaie, A. R. (1999). *J. Biol. Chem.* **274**, 4970–4976.
Hippenmeyer, P. & Highkin, M. (1993). *Nat. Biotechnol.* **11**, 1037–1041.
Joosten, R. P., Joosten, K., Cohen, S. X., Vriend, G. & Perrakis, A. (2011). *Bioinformatics*, **27**, 3392–3398.
Joosten, R. P., Long, F., Murshudov, G. N. & Perrakis, A. (2014). *IUCrJ*, **1**, 213–220.
Korolev, S., Dementieva, I., Sanishvili, R., Minor, W., Otwinowski, Z. & Joachimiak, A. (2001). *Acta Cryst.* D**57**, 1008–1012.
Kuzmič, P. (2009). *Methods Enzymol.* **467**, 247–280.
Laemmli, U. K. (1970). *Nature*, **227**, 680–685.
Le Grand, S., Götz, A. W. & Walker, R. C. (2013). *Comput. Phys. Commun.* **184**, 374–380.
Li, P. & Merz, K. M. Jr (2014). *J. Chem. Theory Comput.* **10**, 289–297.
Li, P., Song, L. F. & Merz, K. M. Jr (2015). *J. Chem. Theory Comput.* **11**, 1645–1657.
Lottenberg, R. & Jackson, C. M. (1983). *Biochim. Biophys. Acta*, **742**, 558–564.
Machius, M., Declerck, N., Huber, R. & Wiegand, G. (1998). *Structure*, **6**, 281–292.
Masys, D. R., Bajaj, S. P. & Rapaport, S. I. (1982). *Blood*, **60**, 1143–1150.
Murshudov, G. N., Skubák, P., Lebedev, A. A., Pannu, N. S., Steiner, R. A., Nicholls, R. A., Winn, M. D., Long, F. & Vagin, A. A. (2011). *Acta Cryst.* D**67**, 355–367.
Navaza, J. (1994). *Acta Cryst.* A**50**, 157–163.
Neuenschwander, P. F., Fiore, M. M. & Morrissey, J. H. (1993). *J. Biol. Chem.* **268**, 21489–21492.

Neuenschwander, P. F. & Morrissey, J. H. (1992). *J. Biol. Chem.* **267**, 14477–14482.
Nonaka, T., Fujihashi, M., Kita, A., Hagihara, H., Ozaki, K., Ito, S. & Miki, K. (2003). *J. Biol. Chem.* **278**, 24818–24824.
Orthner, C. L. & Kosow, D. P. (1978). *Arch. Biochem. Biophys.* **185**, 400–406.
Orthner, C. L. & Kosow, D. P. (1980). *Arch. Biochem. Biophys.* **202**, 63–75.
Otwinowski, Z. & Minor, W. (1997). *Methods Enzymol.* **276**, 307–326.
Padmanabhan, K., Padmanabhan, K. P., Tulinsky, A., Park, C. H., Bode, W., Huber, R., Blankenship, D. T., Cardin, A. D. & Kisiel, W. (1993). *J. Mol. Biol.* **232**, 947–966.
Petrovan, R. J. & Ruf, W. (2000). *Biochemistry*, **39**, 14457–14463.
Price, P. A., Otsuka, A. A., Poser, J. W., Kristaponis, J. & Raman, N. (1976). *Proc. Natl Acad. Sci. USA*, **73**, 1447–1451.
Radcliffe, R. & Nemerson, Y. (1976). *J. Biol. Chem.* **251**, 4749–4802.
Rezaie, A. R. & He, X. (2000). *Biochemistry*, **39**, 1817–1825.
Ruf, W., Rehemtulla, A., Morrissey, J. H. & Edgington, T. S. (1991). *J. Biol. Chem.* **266**, 2158–2166.
Schmidt, A. E., Padmanabhan, K., Underwood, M. C., Bode, W., Mather, T. & Bajaj, S. P. (2002). *J. Biol. Chem.* **277**, 28987–28995.
Schmidt, A. E., Stewart, J. E., Mathur, A., Krishnaswamy, S. & Bajaj, S. P. (2005). *J. Mol. Biol.* **350**, 78–91.
Segal, I. H. (1975). *Enzyme Kinetics: Behavior and Analysis of Rapid Equilibrium and Steady State Enzyme Systems*. New York: John Wiley & Sons.
Shannon, R. D. (1976). *Acta Cryst.* A**32**, 751–767.
Soriano-Garcia, M., Padmanabhan, K., De Vos, A. M. & Tulinsky, A. (1992). *Biochemistry*, **31**, 2554–2566.
Sichler, K., Banner, D. W., D'Arcy, A., Hopfner, K. P., Huber, R., Bode, W., Kresse, G. B., Kopetzki, E. & Brandstetter, H. (2002). *J. Mol. Biol.* **322**, 591–603.
Steiner, S. A. & Castellino, F. J. (1985). *Biochemistry*, **24**, 609–617.
Straume, M. & Johnson, M. L. (1992). *Methods Enzymol.* **210**, 87–105.
Stubbs, M. T. & Bode, W. (1993). *Thromb. Res.* **69**, 1–58.
Underwood, M. C., Zhong, D., Mathur, A., Heyduk, T. & Bajaj, S. P. (2000). *J. Biol. Chem.* **275**, 36876–36884.
Vadivel, K., Agah, S., Messer, A. S., Cascio, D., Bajaj, M. S., Krishnaswamy, S., Esmon, C. T., Padmanabhan, K. & Bajaj, S. P. (2013). *J. Mol. Biol.* **425**, 1961–1981.
Vadivel, K., Schreuder, H. A., Liesum, A., Schmidt, A. E., Goldsmith, G. & Bajaj, S. P. (2019). *J. Thromb. Haemost.* **17**, 574–584.
Waxman, E., Ross, J. B. A., Laue, T. M., Guha, A., Thiruvikraman, S. V., Lin, T. C., Konigsberg, W. H. & Nemerson, Y. (1992). *Biochemistry*, **31**, 3998–4003.
Winn, M. D., Ballard, C. C., Cowtan, K. D., Dodson, E. J., Emsley, P., Evans, P. R., Keegan, R. M., Krissinel, E. B., Leslie, A. G. W., McCoy, A., McNicholas, S. J., Murshudov, G. N., Pannu, N. S., Potterton, E. A., Powell, H. R., Read, R. J., Vagin, A. & Wilson, K. S. (2011). *Acta Cryst.* D**67**, 235–242.
Yamamoto, M., Nakagaki, T. & Kisiel, W. (1992). *J. Biol. Chem.* **267**, 19089–19094.
Zhang, E. & Tulinsky, A. (1997). *Biophys. Chem.* **63**, 185–200.
Zhong, D., Bajaj, M. S., Schmidt, A. E. & Bajaj, S. P. (2002). *J. Biol. Chem.* **277**, 3622–3631.